ARTICLE

Tideglusib attenuates growth of neuroblastoma cancer stem/progenitor cells in vitro and in vivo by specifically targeting GSK-3β

Hisham F. Bahmad[1,2,5] · Reda M. Chalhoub[1,6] · Hayat Harati[2] · Jolie Bou-Gharios[1,2] · Sahar Assi[1] · Farah Ballout[1] · Alissar Monzer[1] · Hiba Msheik[1] · Tarek Araji[1] · Mohamad K. Elajami[1,7] · Paola Ghanem[1] · Farah Chamaa[1] · Humam Kadara[3] · Tamara Abou-Antoun[4] · Georges Daoud[1] · Youssef Fares[2] · Wassim Abou-Kheir[1]

Abstract

Background Neuroblastoma (NB) is the most frequently diagnosed extracranial solid tumor among the pediatric population. It is an embryonic tumor with high relapse rates pertaining to the presence of dormant slowly dividing cancer stem cells (CSC) within the tumor bulk that are responsible for therapy resistance. Therefore, there is a dire need to develop new therapeutic approaches that specifically target NB CSCs. Glycogen synthase kinase (GSK)-3β is a serine/threonine kinase that represents a common signaling node at the intersection of many pathways implicated in NB CSCs. GSK-3β sustains the survival and maintenance of CSCs and renders them insensitive to chemotherapeutic agents and radiation.

Methods In our study, we aimed at evaluating the potential anti-tumor effect of Tideglusib (TDG), an irreversible GSK-3β inhibitor drug, on three human NB cell lines, SK-N-SH, SH-SY5Y, and IMR-32.

Results Our results showed that TDG significantly reduced cell proliferation, viability, and migration of the NB cells, in a dose- and time-dependent manner, and also significantly hindered the neurospheres formation eradicating the self-renewal ability of highly resistant CSCs. Besides, TDG potently reduced CD133 cancer stem cell marker expression in both SH-SY5Y cells and G1 spheres. Lastly, TDG inhibited NB tumor growth and progression in vivo.

Conclusion Collectively, we concluded that TDG could serve as an effective treatment capable of targeting the NB CSCs and hence overcoming therapy resistance. Yet, future studies are warranted to further investigate its potential role in NB and decipher the subcellular and molecular mechanisms underlying this role.

Keywords Neuroblastoma · GSK-3β · Tideglusib · Cancer stem cells · Targeted therapy

Hisham F. Bahmad, Reda M. Chalhoub and Hayat Harati have contributed equally to this work as co-first authors.

Georges Daoud, Youssef Fares and Wassim Abou-Kheir have contributed equally to this work as joint senior authors.

Electronic supplementary material The online version of this article (https://doi.org/10.1007/s43440-020-00162-7) contains supplementary material, which is available to authorized users.

✉ Georges Daoud
gd12@aub.edu.lb

✉ Youssef Fares
yfares@ul.edu.lb

Extended author information available on the last page of the article

Introduction

Neuroblastoma (NB) is the most frequently diagnosed extracranial solid tumor in the pediatric population [1]. It accounts for around 15% of all cancer types diagnosed in children less than 15 years of age in the United States (US) [2]. It is a common tumor of the youngsters that arises from neural crest cells in the embryo, from which the sympathetic nervous system develops [3, 4]. This disease has variable clinical stages based on the patient's clinical characteristics and presentation, pathological and imaging parameters, as well as response to therapy and disease course [5]. Whereas some patients have their tumors spontaneously regress after treatment, others develop resistance to conventional chemo-radiotherapy and progress to metastatic disease stages [4, 6]. Current therapeutic approaches in NB rely on surgery, radiation therapy, and/or chemotherapy [7]. Despite the high

rates of overall 5-year survival among NB patients in the US, reaching up to 80% [8], almost half of those having high-risk disease (i.e. stage 4, amplified MYCN) will suffer from tumor recurrence and unfortunately might not survive long [5, 6].

It has been postulated that tumor relapse after clinical remission in NB and many other tumor types is attributed to the presence of a subpopulation of cells within the bulk of the tumor, known as cancer stem cells (CSC) [9]. These cells are characterized by self-renewal, multipotency, limitless proliferation, and angiogenic and immune evasion features [10]. Conventional therapy usually fails to completely eradicate those therapy-resistant cells and are thus responsible for tumor relapse due to the expression of DNA repair mechanisms, detoxifying enzymes, anti-apoptosis proteins and multiple drug resistance transporters [11, 12]. Indeed, it is hypothesized that those cells play a central role in the initiation, growth, and recurrence of many cancers [13]. Several studies showed that CSCs play a crucial role in NB disease progression, relapse, and poor prognosis [14]. High-risk NBs consist of small populations of cells with preserved stemness characteristics that exhibit the ability to form highly resistant tumorospheres and have high metastatic potential [15]. NB-CSCs are identified based on morphology, cell efflux property, cell surface markers, and tumorosphere formation in in vitro conditions. Identifying specific surface markers is useful for characterization of CSCs and therapeutic targeting. Several markers have been used for NB-CSCs including CD133, frizzled class receptor 6 (FZD6), leucine rich repeat containing GPCR 5 (LGR5), aldehyde dehydrogenase (ALDH), ALDH1A2, ALDH1A3, cluster of differentiation 114 (CD114), and cluster of differentiation 117 (C-kit) [16–18]. Henceforth, there is a dire need to come up with novel targeted therapies capable of eradicating NB-CSCs in order to overcome therapy resistance and subsequently prevent tumor relapse.

In NB, various signaling pathways have been shown to contribute to tumor formation and progression, including but not limited to "canonical" and "non-canonical" Wnt signaling, PI3K/AKT cell survival, hedgehog (SHH) signaling, NF-κB, and MAPK [19], many of which are implicated in the maintenance of CSC [20]. Glycogen Synthase Kinase 3 beta (GSK-3β), which is an active proline-directed serine/threonine kinase, is a key player and common node at the intersection of many of the aforementioned pathways [21]. However, different research studies have demonstrated its controversial role in cancer. For example, GSK-3β has multifaceted roles in Wnt signaling: while its inhibition mediates β-catenin phosphorylation and activates Wnt/β-catenin signaling, roles of GSK3-β in the β-catenin-independent signaling pathway demonstrate differential effects [22]. Also, although GSK-3β has been long appreciated as a tumor suppressor, such as in colon cancer where it activates

adenomatous polyposis coli (APC)-β-catenin destruction complex, recent studies have highlighted its potential role as a target protein for other tumor types, including pancreatic adenocarcinoma and acute myeloid leukemias [23–26]. Evidence suggests that GSK-3β is a tumor promoter in glioma where its inhibition has been associated with decreased proliferation, inhibited cell survival, enhanced tumor cell apoptosis and differentiation, impaired formation of neurospheres, and reduced clonogenicity [27]. GSK-3β activation was also identified as a key element in maintaining stem cell-like characteristics in a subset of glioma cells, providing these cells with a higher self-renewal capacity. These findings suggest that GSK-3β inhibitors might serve as potential treatment modalities for NB.

Inhibition of GSK-3β has been previously tackled in NB where various inhibitors have been shown to induce apoptosis of NB cells via activating the canonical Wnt signaling pathway in a p53-independent manner [28]. However, no studies have been conducted yet to test the effect of GSK-3β on NB-CSCs specifically. Herein, we aimed to assess the anti-tumor effects of Tideglusib (TDG), a specific GSK-3β inhibitor, on NB-CSCs in vitro and in vivo (Fig. 1). This drug was specifically chosen among many other inhibitors since it is well-tolerated and causes an irreversible non-ATP competitive GSK-3β inhibition [29]. In addition, it was previously clinically assessed and shown to have promising therapeutic advantages in treating neurological disorders, such as Alzheimer's disease and progressive supranuclear palsy [30–32]. Our results showed that treating human NB cell lines with TDG inhibited cell viability, reduced migration, and further hindered 3D neurosphere formation and propagation over sequential generations of neurospheres in vitro. Besides, TDG potently reduced NB tumor growth and progression in vivo.

Materials and methods

Cell culture and treatment

In our study, three NB cell lines were used: SK-N-SH (ATCC® HTB-11™, USA; RRID:CVCL_0531) [33], SH-SY5Y (ATCC® CRL-2266™, USA; RRID:CVCL_0019) [34, 35], and IMR-32 (ATCC® CCL-127™, USA; RRID:CVCL_0346) [36]. Cells were cultivated and maintained in Dulbecco's Modified Eagle Media (DMEM) Ham's F12 (Sigma-Aldrich; cat #D8437) medium, supplemented with 10% of heat inactivated fetal bovine serum (FBS) (Sigma-Aldrich; cat #F9665), 1% Penicillin/Streptomycin (Biowest; cat #L0022-100) and Plasmocin™ prophylactic (Invivogen; cat #ant-mpp). By checking the cell lines using the "International Cell Line Authentication Committee" (ICLAC) database of cross-contaminated or misidentified

Increased expression of GSK-3β in Neuroblastoma

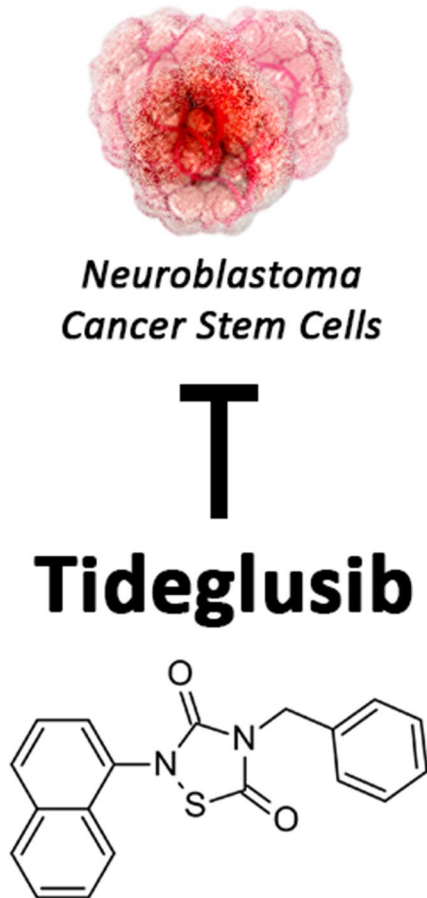## Neuroblastoma Cancer Stem Cells

Tideglusib

Fig. 1 Schematic illustrating potential anti-tumor effect of Tideglusib (TDG), an irreversible GSK-3β inhibitor drug, on targeting neuroblastoma tumor

cell lines, we confirmed that the three cell lines are not misidentified or contaminated. Cells were incubated at 37 °C in a humidified incubator containing 5% CO_2. Tideglusib (TDG) was purchased from Sigma-Aldrich (cat #SML0339-10MG; Lot # 123M4615V and 016M4605V) and reconstituted in dimethyl suldoxide (DMSO; Amresco; cat #0231-500ML), per manufacturer's instructions.

MTT/cell proliferation assay

To measure the in vitro anti-proliferative effects of Tideglusib (TDG) on the used cell lines, MTT ([3-(4, 5-dimethylthiazol-2-yl)-2,5-diphenyltetrazolium bromide]) (Sigma-Aldrich; cat #M5655-1G) cell proliferation assay was used and manufacturer's instructions were followed [37–39]. This tetrazolium reduction assay was the first homogeneous

cell viability assay developed [38], where MTT reacts with NADH or similar reducing molecules through specific mitochondrial enzymes within the viable cells having active metabolism. This allows for transfer of electrons to MTT that subsequently converts from a yellow colored agent into a purple colored formazan product [40].

Cells were seeded at a density of 6×10^3 cells in 100 μL full media, per well, in three 96-well culture plates (one for every time point: 24 h, 48 h and 72 h) and incubated overnight at 37 °C and 5% CO_2. Three wells were prepared for each treatment condition and randomly distributed across the different conditions (Control: media only, Vehicle: Media + 0.1% DMSO, treatment groups: 5 μM, 25 μM, and 50 μM TDG in full media). At every time point, media was removed and replaced with fresh media along with 10μL of MTT yellow dye (5 mg/mL in DMSO) per well. Cells were then incubated for 4 h and 100μL of the solubilizing agent was added to each well. The plates were incubated overnight at room temperature, and the absorbance intensity of every well was measured by the microplate ELISA reader (Multiscan EX) at 595 nm. The percentage of cell proliferation was presented as an optical density (OD) ratio of the treated to the untreated cells (control).

Trypan blue/cell viability assay

To further validate the anti-tumor effects of TDG on cell viability in vitro, trypan blue assay was used as previously described [41]. This assay is a simple method to measure cell viability in cell culture based on counting the number of viable cells using the trypan blue dye. Since non-viable dead cells in culture with disrupted cell membranes allow trypan blue dye to be taken up, only viable cells can be visualized under the microscope as white cells while non-viable dead cells are stained blue [41].

SH-SY5Y and SK-N-SH cells were seeded in three different 12-well culture plates (one for each time point: 24 h, 48 h, and 72 h) at a density of 60×10^3 cells/well in 500 μL full media. Cells were incubated overnight at 37 °C and 5% CO_2. Wells were prepared, in duplicate, and randomly distributed across the same treatment conditions as described in the previous section under 'MTT/Cell Proliferation Assay'. At every time point, cells from each well were detached using trypsin–EDTA solution (Sigma-Aldrich; cat #T4049), then fresh growth medium was added to neutralize trypsin and viable cells were counted on a hemocytometer under an inverted light microscope after staining cell suspension with Trypan blue. The percentage of cell viability was determined as a ratio of viable cells counted in treated to untreated conditions.

Wound healing assay

Wound healing assay was then used to assess the effects of TDG on cell migration. Wound healing cell migration assay is also known as scratch assay and it is a simple method to assess directional cell migration in vitro. It is one of the earliest developed methods that resemble cell migration occurring in the process of wounds' healing in vivo [42].

In our study, SH-SY5Y and SK-N-SH cells were seeded in 6-well culture plates at a density of 5×10^5 cells/well and incubated at 37 °C and 5% CO_2 until they reached 90% confluence. Cells were then treated with 5 mg/mL of Mitomycin C (Sigma-Aldrich; cat #M0503-5x2MG) for 1 h to block cellular proliferation and to assure that closure of the wound is a function of cellular migration and not cellular proliferation. Two uniform scratches of the same width were made per well in each monolayer using a sterile 200 µL micropipette tip and the plates were then washed twice with dulbecco's phosphate buffered saline (D-PBS) (Sigma-Aldrich; cat #D8537-500ML) to remove the detached cells and any cell debris. The remaining cells were cultured in complete growth media with or without treatment. Three conditions were considered here: control (full media), vehicle (full media + 0.1% DMSO), and treatment (25 µM TDG in full media). Markings were created thereafter on the backside of the plate using a marker, to serve as reference points in order to obtain the same field during image taking process. Pictures of the scratches were taken using an inverted light microscope at the following time points: 0 h, 6 h, 12 h, 24 h, and 48 h. At every selected time point, wells were washed once with PBS to remove any dead and floating cells. The distance travelled by the cells was measured using Zen Microscope Software (Zen 2.3). The distance traveled by the cells was computed from the closure of the wounds and expressed as percentage of the wound closure upon treatment compared to the control.

3D culture and sphere-formation assay

The sphere formation assay was performed as previously reported by our group [43–46]. In brief, single SH-SY5Y and SK-N-SH cell suspensions were seeded in growth factor-reduced Matrigel™/serum free DMEM Ham's F-12 (1:1) at a density of 2×10^3 cells/well. The solution was then plated gently around the rim of individual wells of 24-well culture plate (50 µL per well). The Matrigel™ (Corning Life Sciences; cat #354230) was allowed to solidify for 1 h at 37 °C in a humidified incubator. Different culture conditions were used here: control, 0.1 µM, 1 µM, and 5 µM TDG. Complete media (+ 5% FBS) at a volume of 500 µL/well was gently added to the center of each well and changed regularly every 2–3 days. At day 9–14 after plating, spheres were pictured and counted. Same protocol was applied on IMR-32 cells.

SH-SY5Y spheres were further harvested for propagation. Several published papers have shown the effects of different drugs, targeting specific signaling pathways, on sphere formation ability of presumably putative CSCs [43–52].

For spheres propagation, the medium was aspirated from the center of the wells. Matrigel™ was digested with 0.5 mL of 1 mg/mL Dispase II solution (ThermoFisher; cat #17105-041) dissolved in serum-free DMEM Ham's F-12 for 1 h at 37 °C in a humidified incubator. SH-SY5Y and SK-N-SH spheres were collected and incubated in warm trypsin–EDTA solution at 37 °C for 5 min; trypsin–EDTA solution was used to dissociate spheres into single cell suspensions. Cells were counted and re-seeded at the same density as used in the first generation (G1) of 2×10^3 cells/ well. The propagation of the spheres was repeated over 4 generations. The sphere forming unit (SFU) was calculated as the ratio of the number of spheres counted at day 9–14 to the number of cells originally seeded. Bright field images of the spheres were obtained using Axiovert microscope from Zeiss at $5 \times$ magnification.

Western blotting analysis

SH-SY5Y cells were seeded at a density of 5×10^5 cells/well and cultured in 6-well plates until they reached 80% cell confluence. Wells were treated, in triplicates, with 25 µM TDG for 48 h, while other wells were taken as control. Cells were then washed with ice-cold D-PBS. SH-SY5Y spheres (G1) were also treated with 5 µM TDG while others were taken as control. G1 spheres were then collected and washed with ice-cold D-PBS. Cells/spheres were treated and lysed using radioimmunoprecipitation (RIPA) buffer (0.1% sodium dodecyl sulfate (SDS) (v/v), 0.5% sodium deoxylate (v/v), 150 mM sodium chloride (NaCl), 100 mM EDTA, 50 mM Tris–HCl (pH 8), 1% Tergitol (NP40) (v/v), 1 mM PMSF, and protease and phosphatase inhibitors [one tablet of each in 10 mL buffer, Roche, Germany]), scraped off the plates, transferred into micro-centrifuge tubes and incubated on ice for 30 min. Sonication was used to maximize the protein yield. Lysates were then centrifuged at 13,600 rpm for 15 min at 4 °C, to pellet the cell debris.

Quantification of the protein concentrations of the collected supernatants was done using DC™ Protein Assay (Bio-Rad). For immunoblotting, 50 µg of proteins were electrophoresed in 8% or 12% polyacrylamide gel and then transferred to PVDF membranes (Bio-Rad Laboratory, CA, USA) overnight. Then, 5% bovine serum albumin (BSA) (v/v) (Amresco; cat #0332-100G) was added for 2 h to block the membranes after which they are blotted at 4 °C overnight with primary antibodies as follows: rabbit anti-GSK-3β (1/1000 dilution; Cell Signaling Technology; cat #9315; RRID:AB_490890), rabbit anti-phospho-GSK-3β (Ser9) (5B3) (1/500 dilution; Cell Signaling Technology;

cat #9323; RRID:AB_2115201), and mouse anti-GAPDH (1/5000 dilution; Novus Biologicals; cat #NB300-221; RRID:AB_10077627). The next day, membranes were washed and incubated at room temperature for 2 h with the appropriate HRP-conjugated secondary antibodies as follows: mouse anti-rabbit (1/1000 dilution; Santa Cruz Biotechnology; cat #sc-2357; RRID:AB_628497) and mouse IgGκ BP (1/1000 dilution; Santa Cruz Biotechnology; cat #sc-516102; RRID:AB_2687626). Finally, bands were detected using Lumi-Light Western Blotting Substrate (Roche; cat #12015200001) and visualized using autoradiography. Quantification of the protein expression was done relative to the expression of GAPDH (housekeeping gene that is equally expressed in treated and non-treated cells/spheres) using Image Lab software (RRID:SCR_014210). Band intensities were digitized and analyzed using ImageJ software (RRID:SCR_003070).

Immunofluorescence staining

Indirect immunofluorescence (IF) analysis was pursued to assess the effect of TDG on CD133 stem cell marker expression in neuroblastoma cells and spheres. Two-dimensional (2D) cells were grown on coverslips and treated with 25 µM TDG for 48 h. Then, adherent cells were fixed using 4% PFA (v/v) in PBS for 20 min and permeabilized with 0.5% Triton X-100 (v/v) in PBS for 20 min. In order to block non-specific sites, cells were incubated in blocking buffer (0.1% BSA (v/v), 0.2% Triton X-100 (v/v), 0.05% Tween-20 (v/v) and 10% NGS (v/v) in PBS) for one hour (bovine serum albumin (BSA) (v/v) (Amresco; cat #0332-100G), normal goat serum (NGS) (v/v) (ThermoFisher; cat #16210064), Tween-20 (Sigma-Aldrich; cat #P1379), and Triton X-100 (v/v) (Sigma-Aldrich; cat #T9284)).

To perform the IF on spheres in suspension, G1 SH-SY5Y spheres untreated and treated with 5 µM TDG were collected. Matrigel™ was dissolved using ice-cold medium. After that, the pellet was fixed in 4% PFA (v/v) for 30 min. Then spheres were permeabilized with 0.5% Triton X-100 (v/v) for 30 min at room temperature, followed by a blocking buffer for 1 h at room temperature as previously described.

Cells and spheres were then incubated overnight with specific primary antibody at 4 °C. The next day, cells and spheres were washed with PBS containing 0.1% Tween-20 (v/v), and incubated with the corresponding secondary antibody, then washed gently and mounted with anti-fade reagent Fluoro-gel II with DAPI (Electron Microscopy Sciences; cat #17985-51). Fluorescent signals were captured using a Zeiss LSM 710 laser scanning confocal microscope (Zeiss, Germany) and images were processed using the Zeiss ZEN 2012 image-analysis software. The following antibodies were used: mouse monoclonal anti-CD133 (1/100 dilution; Cell Signaling Technology; cat #5860; RRID:AB_2797621) and secondary Alexa Fluor 568 goat anti-mouse IgG (1/200 dilution; ThermoFisher; cat #A-11004). Fluoro-gel II with DAPI (Electron Microscopy Sciences, PA) was used for mounting.

Mouse neuroblastoma xenografts

Prior to commencement of any experiments on animals, all applicable international, national, and institutional guidelines that are specific to animal care and use were followed. Approval of the Institutional Animal Care and Utilization Committee (IACUC) of the American University of Beirut was also obtained. In our study, we followed the ARRIVE guidelines (https://www.nc3rs.org.uk/arrive-guidelines) for animal researches. Neuroblastoma xenografts were generated using mouse SH-SY5Y cells. Cells were injected at a density of 1.2×10^6 cells in 100 µL total volume of Matrigel™/serum free DMEM Ham's F-12 (1:1) using a 27 G needle subcutaneously, into the flanks of NOD-SCID male mice (6–8 weeks old) [53]. When a palpable tumor (approximate size 1mm^3) was detected, mice were intraperitoneally injected 3 times per week with 20 mg/kg TDG or vehicle only (Lipofundin/DMSO) for a period of 2 weeks. Tumor volumes were measured every 3 days by direct physical measurements using a digital caliper (Model DC150-S). Weight of the mice was determined at the beginning of the experiment and at the time of sacrifice of mice. To assess tumor volume, the following formula was applied: $V = (3.14/6) \times L \times W \times H$; where V is the tumor volume in mm^3, L is the tumor length in mm, W is the tumor width in mm, and H is the tumor height in mm. Measurements were performed until the termination of the animal experiments. Data represent an average of $n = 3$ mice. The data are reported as mean $\pm$ SEM.

Statistical analyses

Statistical analyses were performed using GraphPad Prism 7 software (RRID:SCR_002798). Data significance was determined using either student t test or two-way ANOVA statistical test, followed by multiple comparisons using Bonferroni post-hoc analysis. For the in vivo experiments, Wilcoxon matched-pairs signed rank test was used. P values of $p < 0.05$ (*), $p < 0.01$ (**) and $p < 0.001$ (***) were labeled significant, highly significant, and very highly significant, respectively.

Results

Expression patterns of GSK-3β mRNA in human neuroblastoma tissues

We first surveyed a publicly available dataset (Neale Multi-cancer Statistics, 60 samples; data retrieved from Oncomine Research Platform; URL: https://www.oncomine.org; RRID:SCR_007834) to assess the mRNA expression patterns of *GSK-3β* gene in human NB tumor tissues compared to cancer tissues from other body organs. Results demonstrated high mRNA expression of *GSK-3β* in NB tumor tissues relative to tumor tissues in three out of four probes of the dataset (fold change = 1.639; $p = 4.06E-4$) (Figs. 2, S1).

TDG reduced cell viability and cell proliferation of SH-SY5Y, SK-N-SH, and IMR-32 cells

We then assessed the in vitro anti-tumor effect of TDG on cell proliferation and viability of human NB cell lines, SK-N-SH and SH-SY5Y, using MTT (Fig. 3a, b) and Trypan Blue (Fig. 3c, d) assays, respectively. Results revealed that treatment with TDG significantly reduced the proliferative ability of SH-SY5Y and SK-N-SH cells in a dose-dependent manner. A 50% inhibitory effect of TDG was achieved at a concentration of 25 μM for both cell lines after 72 h (Fig. 3a, b). For further validation, we observed a significant

inhibitory effect of TDG treatment on cell viability using trypan blue exclusion assay (Fig. 3c, d). As a proof of principle, effect of TDG was assessed on proliferation of another human NB cell line, IMR-32, revealing significant dose- and time-dependent inhibition upon treatment for 72 h (Figure S2).

TDG hindered cell migration of human NB cells in vitro

Knowing that neuroblastoma could be exceptionally aggressive in nature and tend to infiltrate the nearby tissues and metastasize [54, 55], we investigated the effect of TDG on cell migration of NB cell lines SH-SY5Y and SK-N-SH using wound healing assay. In the control conditions, cells were able to migrate and almost close the wounds completely within 48 h. However, upon treatment with 25 μM TDG, the wound made in SH-SY5Y and SK-N-SH monolayers remained patent by 60% and 70%, respectively (Fig. 4). This shows that TDG effectively impedes migration of NB cells in vitro.

TDG reduced the neurosphere formation of SH-SY5Y, SK-N-SH, and IMR-32 cells

SH-SY5Y cells were cultivated, by single cell suspensions, in Matrigel™-based 3D cultures under non-adherent conditions for 9–14 days and allowed to form neurospheres. Sphere
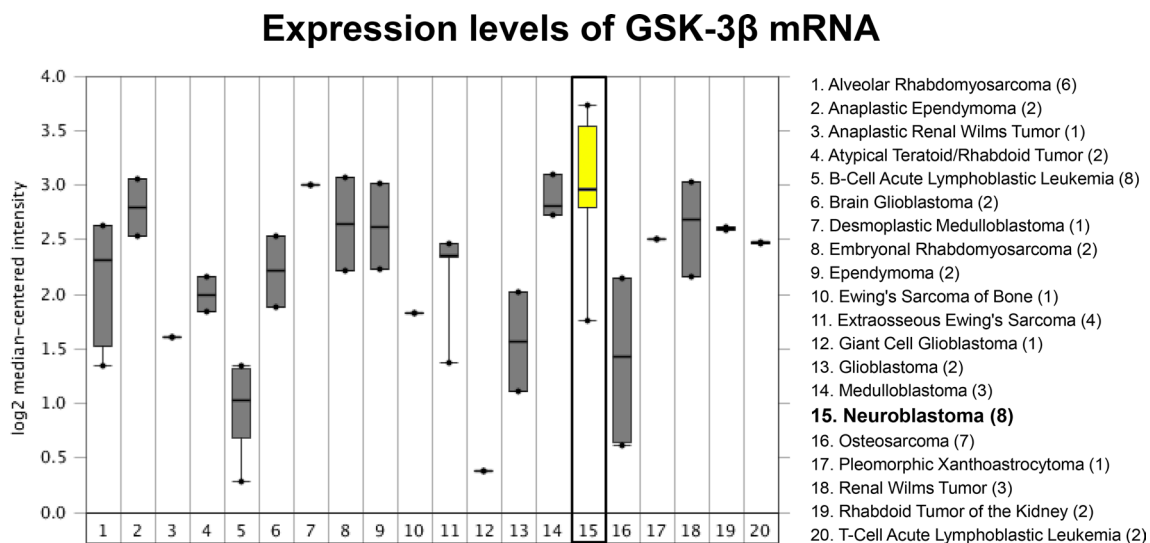

Expression levels of GSK-3β mRNA

1. Alveolar Rhabdomyosarcoma (6)
2. Anaplastic Ependymoma (2)
3. Anaplastic Renal Wilms Tumor (1)
4. Atypical Teratoid/Rhabdoid Tumor (2)
5. B-Cell Acute Lymphoblastic Leukemia (8)
6. Brain Glioblastoma (2)
7. Desmoplastic Medulloblastoma (1)
8. Embryonal Rhabdomyosarcoma (2)
9. Ependymoma (2)
10. Ewing's Sarcoma of Bone (1)
11. Extraosseous Ewing's Sarcoma (4)
12. Giant Cell Glioblastoma (1)
13. Glioblastoma (2)
14. Medulloblastoma (3)
15. **Neuroblastoma (8)**
16. Osteosarcoma (7)
17. Pleomorphic Xanthoastrocytoma (1)
18. Renal Wilms Tumor (3)
19. Rhabdoid Tumor of the Kidney (2)
20. T-Cell Acute Lymphoblastic Leukemia (2)

Fig. 2 Expression levels of *GSK-3β* mRNA were assessed in an array set comprised of human pan-tumor samples (Neale Multi-cancer Statistics, Reporter 226183_at is presented; the remaining probes of the dataset are presented in Figure S1: Reporters 209945_s_at, 226191_at, and 242336_at). Expression within tumor tissues was presented by log (base 2) median-centered expression of *GSK-3β*. Box and whiskers plots indicate median and interquartile range. p values were obtained using *t*-tests (Neale Multi-cancer Statistics, 60 samples; data retrieved from Oncomine Research Platform; URL: https://www.oncomine.org; RRID:SCR_007834). Analysis revealed that mRNA expression of *GSK-3β* gene was the highest among neuroblastoma tissues relative to other organ specific tumor tissues (fold change = 1.639; $p = 4.06E-4$)
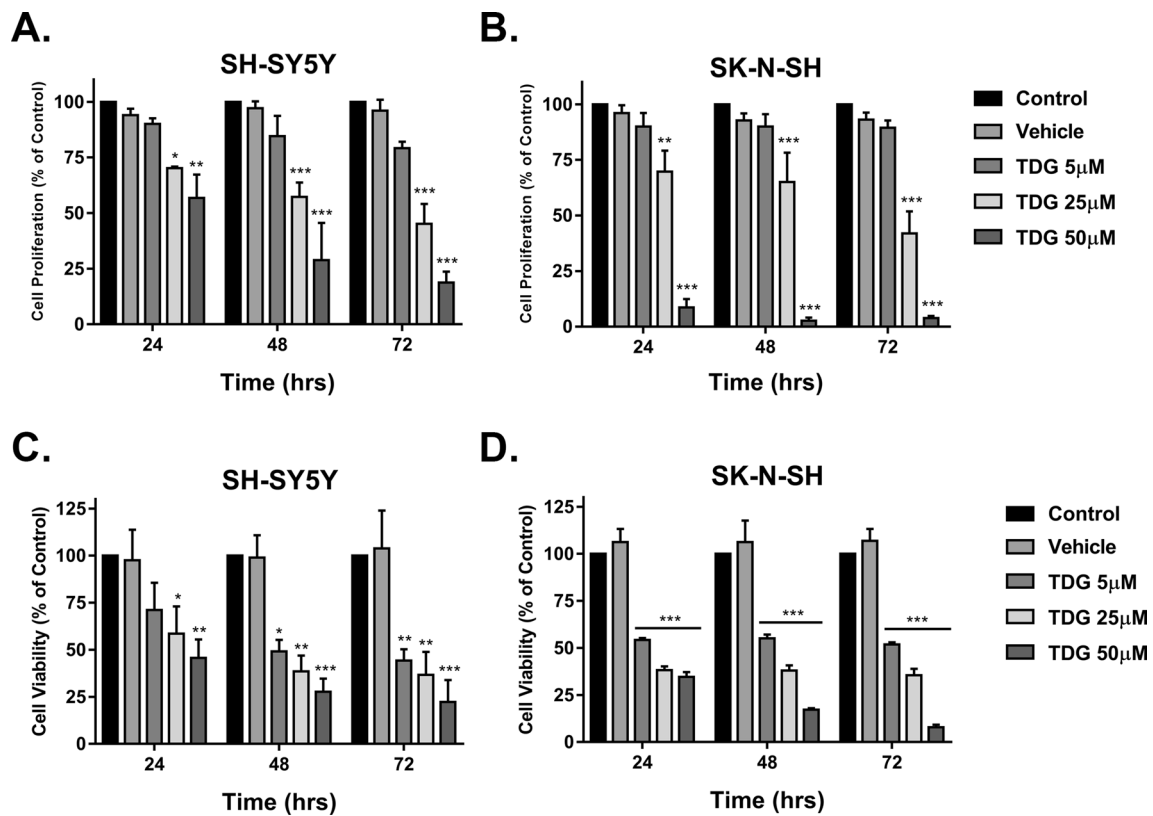
Fig. 3 Tideglusib significantly decreases cell proliferation and cell viability of human neuroblastoma cells. **a** The effect of TDG on cell proliferation was determined using the MTT assay. Tideglusib significantly decreases cell proliferation of SK-N-SH (two-way ANOVA; treatment $F_{4,30} = 143$, $p < 0.001$; time $F_{2,30} = 2.02$, $p = 0.15$; interaction $F_{8,30} = 1.29$, $p = 0.2858$) and SH-SY5Y (two-way ANOVA; treatment $F_{4,30} = 50.78$, $p < 0.001$; time $F_{2,30} = 5.801$, $p = 0.0074$; interaction $F_{8,30} = 1.738$, $p = 0.1303$) cells in dose-dependent manner, as determined by MTT. **b** The effect of TDG on cell viability was deter-

mined using the trypan blue assay. Tideglusib significantly decreases the percentage of viable cells in SK-N-SH (two-way ANOVA; treatment $F_{4,30} = 248.5$, $p < 0.001$; time $F_{2,30} = 2.791$, $p = 0.0773$; interaction $F_{8,30} = 2.002$, $p = 0.0808$) and SH-SY5Y (two-way ANOVA; treatment $F_{4,30} = 25.22$, $p < 0.001$; time $F_{2,30} = 2.16$, $p = 0.1329$; interaction $F_{8,30} = 0.524$, $p = 0.8289$) cells in dose-dependent manner, as determined by MTT. The data are reported as mean ± SEM of three independent experiments. Bonferroni post-hoc analysis was done to determine simple factor effects. (*$p < 0.05$, **$p < 0.01$, ***$p < 0.001$)

formation was examined daily using an inverted light microscope, and pictures were taken to assess the size and shape of formed neurospheres. Sphere formation assay is a functional assay used herein to study the stem/progenitor cells subpopulation within SH-SY5Y cells. Treating cells that are embedded in Matrigel™ with TDG significantly hindered neurospheres formation and decreased the SFU (one-way ANOVA, $p = 0.0037$) (Fig. 5a, b) and average sphere volume (one-way ANOVA, $p < 0.001$) (Fig. 5c) in a dose-dependent manner. Noteworthy, much lower concentrations of the drug were sufficient to instigate an inhibitory anti-tumor effect in 3D cultures compared to functional assays in 2D monolayers. For further validation, spheres formation assay was performed on

SK-N-SH cells and results were consistent with that observed with SH-SY5Y. Indeed, we observed a significant decrease in SFUs at G1 spheres in a dose-dependent manner (one-way ANOVA, $p < 0.001$) (Figure S3A). As a principle of proof, effect of TDG was assessed on sphere formation ability of IMR-32 human NB cells showing a significant dose-dependent decrease in SFU at G1 spheres (Figure S4).
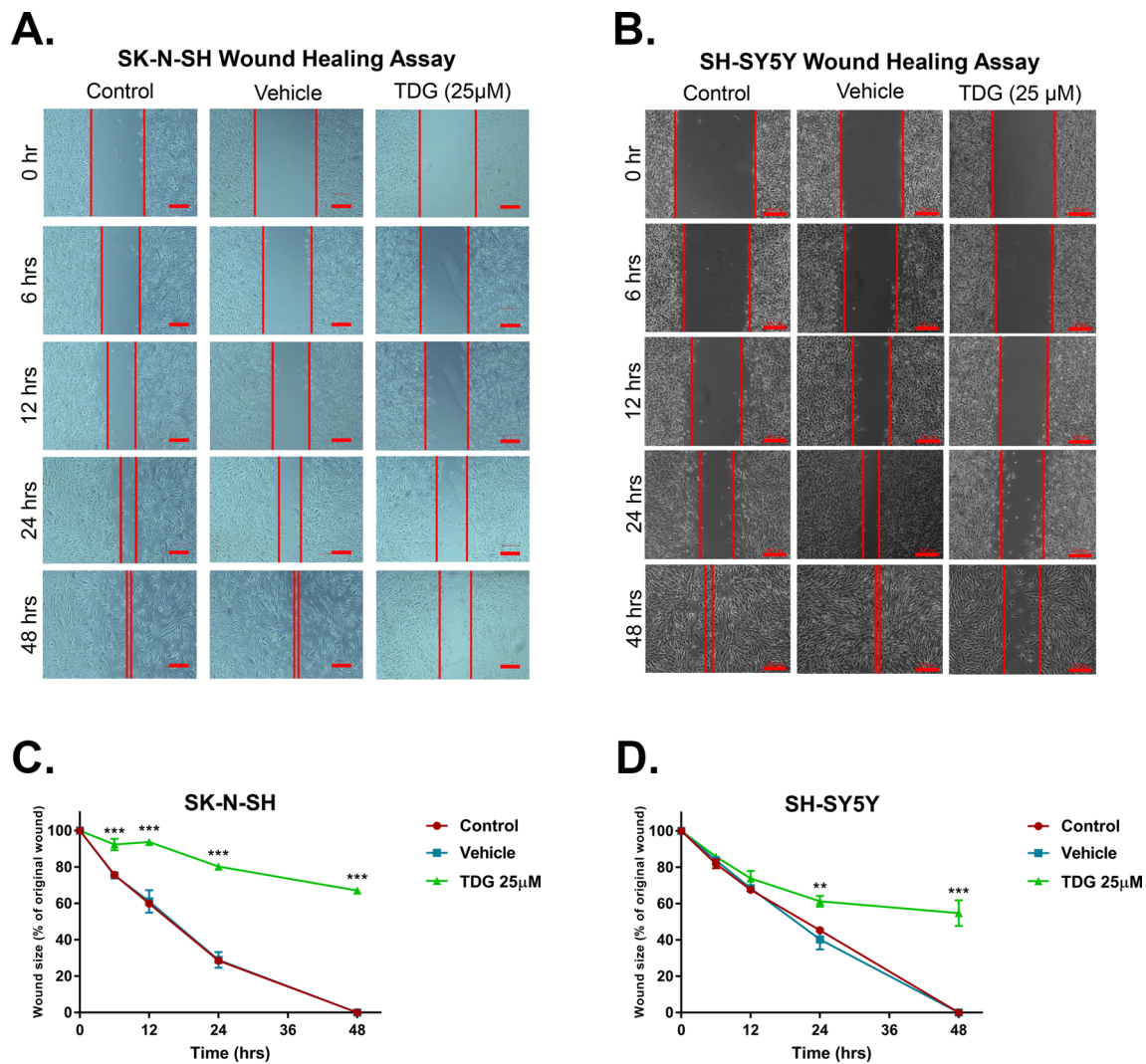
Fig. 4 Tideglusib inhibits cell migration of SK-N-SH and SH-SY5Y human neuroblastoma cells. Representative figures showing the scratch made in SK-N-SH (**a**) and SH-SY5Y (**b**) cell lines at five different timepoints: 0 h, 6 h, 12 h, 24 h and 48 h. These figures show closure of the wound after 48 h in control and vehicle treated conditions as opposed to the TDG (25 μM) treated conditions. Scale = 200 μm in **a** and 100 μm in **b**. A scratch was made to cells seeded in 6-well plates at $T=0$ h using a 200μL pipet tip; distances between cells were assessed at the different timepoints to determine the drug's effects on cellular migration. The data are reported as percentages of the distance between cells relative to original wound size at $T=0$ h. Tideglusib (25 μM) significantly inhibited cell migration of SK-N-SH (**c**) (two-way ANOVA with repeated measures: treatment $F_{2,6}=1659$, $p<0.001$; time $F_{4,24}=454.3$, $p<0.001$; interaction $F_{8,24}=38.83$, $p<0.001$) and SH-SY5Y (**d**) (two-way ANOVA with repeated measures: treatment $F_{2,6}=80.98$, $p<0.001$; time $F_{4,24}=340.8$, $p<0.001$; interaction $F_{8,24}=19.29$, $p<0.001$) cell lines, in a dose- and time- dependent manners. The data are reported as mean ± SEM of three independent experiments. Bonferroni post-hoc analysis was done to determine simple factor effects. (**$p<0.01$, ***$p<0.001$ when compared to control)

TDG inhibited the self-renewal ability of NB by targeting an enriched population of SH-SY5Y and SK-N-SH cancer stem/progenitor cells

To investigate the self-renewal ability (which is a major characteristic of CSCs largely responsible of cancer recurrence) of stem/progenitor cells, we assessed the effect of TDG on the neurosphere forming capability by propagating SH-SY5Y and SK-N-SH spheres over multiple generations. Cells taken from one generation of spheres were isolated into single cell suspensions and seeded again in Matrigel™-based 3D cultures. Propagating spheres into consecutive generations is thought to enrich the cancer stem/progenitor cells subpopulation, by accentuating their anchorage-independent growth ability [48]. Figures 5d and S3B demonstrate the experimental design and results of experiments performed in triplicates for SH-SY5Y and SK-N-SH neurospheres, respectively. Notably, treating G4
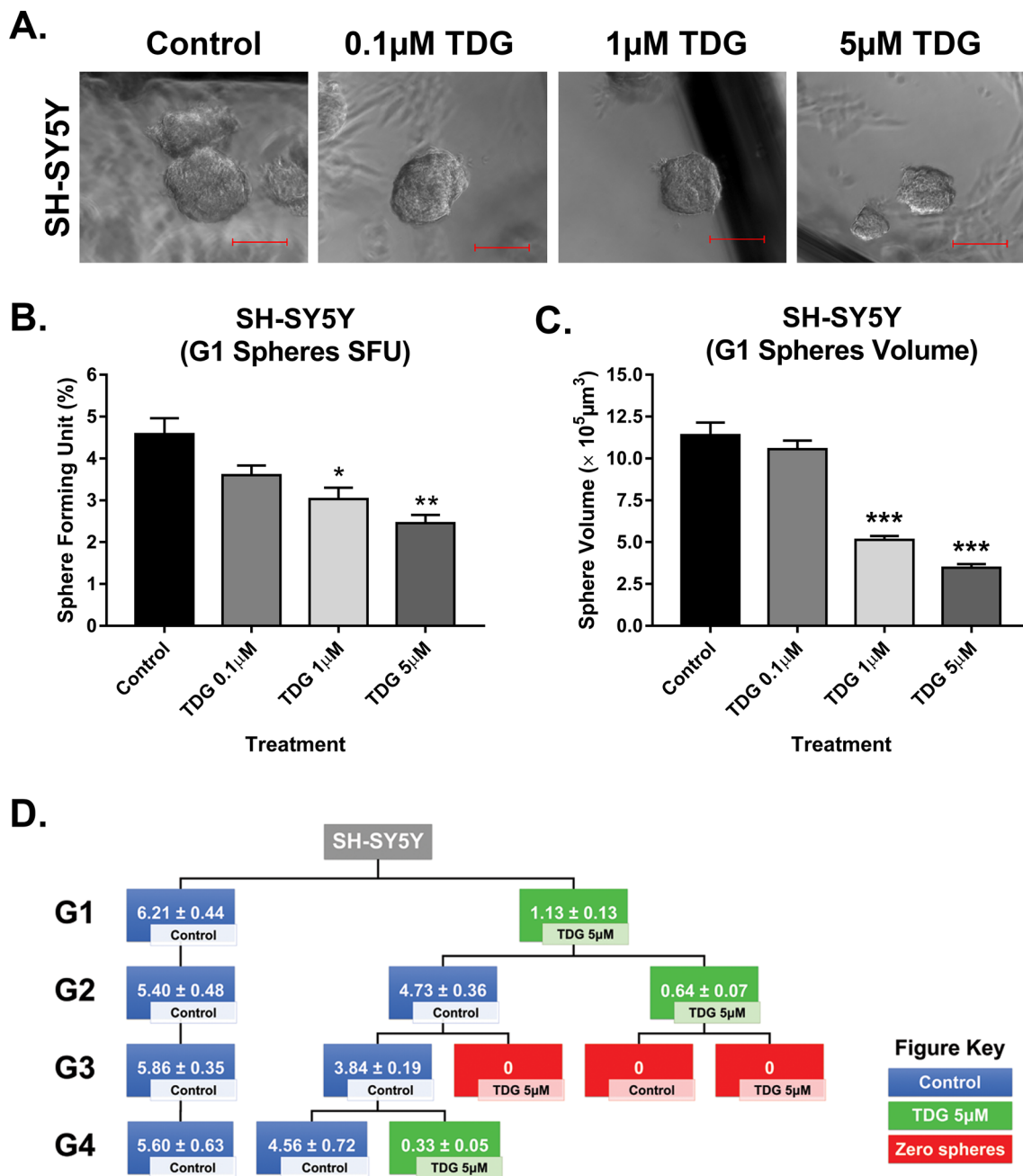
Fig. 5 Tideglusib effectively decreases the percentage of self-forming units and volume of spheres and targets an enriched cancer stem/progenitor subpopulation in the sphere formation assay on SH-SY5Y cells. **a** Representative images taken of SH-SY5Y spheres under different conditions (control, 0.1 µM TDG, 1 µM TDG and 5 µM TDG) using inverted light microscopy showing the gradual decrease in size of spheres in treatment dose-dependent manner. **b** Tideglusib decreases the percentage of SFUs in SH-SY5Y cell suspensions in a dose-dependent manner (one-way ANOVA followed by Bonferroni multiple comparisons: treatment $F_{3,8} = 10.6$, $p = 0.0037$). **c** TDG treatment decreases the volume of the formed spheres in a dose-dependent manner (one-way ANOVA followed by Bonferroni multiple comparisons: treatment $F_{3,356} = 66.27$, $p < 0.001$). The data are reported as mean $\pm$ SEM of three independent experiments. Bonferroni post-hoc analysis was done to determine simple factor effects (*$p < 0.05$, **$p < 0.01$ and ***$p < 0.001$ when compared to control). **d** Schematic summarizing the experimental design and results of serial propagation of spheres across 4 generations. Spheres from control and treated conditions were isolated, dissociated into single cell suspensions and seeded under non-adherent conditions. Wells were then randomly distributed into treated and non-treated conditions to assess the effect of treatment across generations. The numbers shown represent the average percentage of SFUs as obtained from three independent experiments. The data was analyzed using multiple independent t tests across each generation

spheres—that have acquired an enriched stem/progenitor subpopulation of cells—with 5 μM of TDG significantly reduced SFU by around 95% for SH-SY5Y cells (student independent *t* test, $p < 0.001$, Figure S5A) and 80% for SK-N-SH cells (student independent *t* test, $p < 0.001$, Figure S5B).

In our experiments, we went a step further with SH-SY5Y neurospheres that were treated with TDG where we tested their self-renewal ability by propagating them into two conditions, control and treated, at each subsequent generation (as shown in Fig. 5d). Results revealed that after a single exposure to 5 μM of TDG at G1, SFU significantly dropped to 1.13% compared to 6.21% in control conditions (student independent *t* test, $p < 0.0001$) (Fig. 5d). However, when those treated neurospheres at G1 were propagated into G2 but under untreated condition, cells were found to

successfully regain their self-renewal ability (SFU = 4.73%). Moreover, consecutive propagation of neurospheres indicated that it takes at least two treatment regimens over two subsequent generations to completely abolish spheres formation, i.e. single cell suspensions from neurospheres previously treated over two successive generations will fail to form any spheres thereafter (Fig. 5d).

TDG inhibited GSK-3β at protein levels

Since TDG acts by specifically targeting GSK-3β and inhibiting it at a subcellular level, we sought to validate its direct effect at a protein level using western blotting. We evaluated the differences in protein expression between cellular lysates in TDG-treated vs. non-treated SH-SY5Y cells and G1 spheres. Inhibition of GSK-3β is established
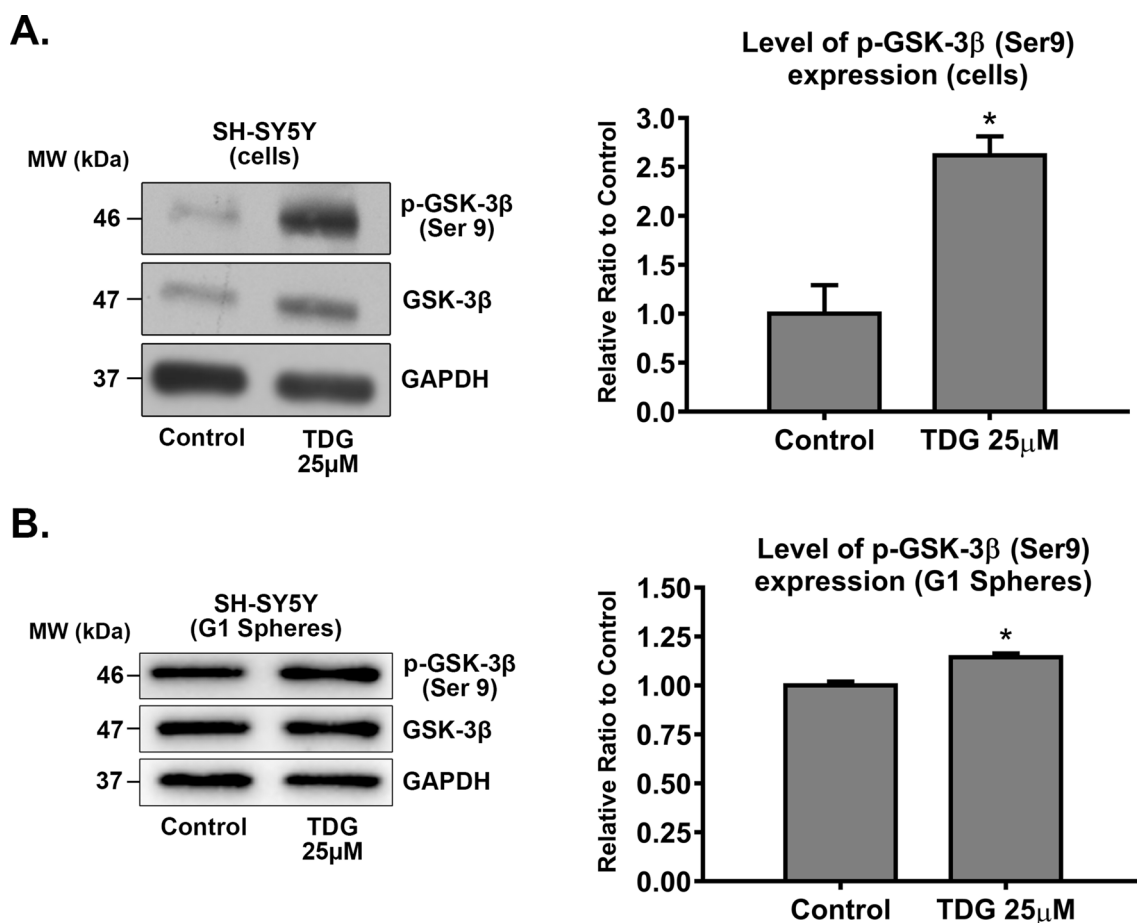

Fig. 6 Tideglusib selectively inhibits GSK-3β by increasing expression of its inhibited form, phosphorylated at Serine 9 (p-GSK-3β Ser 9). After treating SH-SY5Y cells with 25 μM TDG (for 48 h) (**a**) and G1 spheres with 5 μM TDG (**b**), proteins were extracted using RIPA buffer, and used to detect differences in expression of the phosphorylated form of GSK-3β (Ser 9). Bands were detected by enhanced chemiluminescence (ECL) using ChemiDoc MP Imaging System. Protein expression was quantified using Image Lab software (RRID:SCR_014210), relative to the expression of GAPDH, a housekeeping gene equally expressed in treated and non-treated cells/spheres. Results are expressed as relative ratio to control. Analysis of p-GSK-3β (Ser 9) protein level was done after normalization with total GSK-3β protein levels. Data represent an average of three independent experiments. The data are reported as mean ± SEM. (*p < 0.05; treatment compared to control, student independent *t* test)

by its phosphorylation at Serine 9 and hence an increase in the levels of expression of the inhibited form, p-GSK-3β (Ser 9). Our results revealed that treating SH-SY5Y cells with 25 μM of TDG significantly increased the expression of p-GSK-3β (Ser 9) by 2.62 times ($p = 0.0102$) compared to the untreated (control condition) (Fig. 6a), signifying GSK-3β inhibition. In addition, treating first generation SH-SY5Y neurospheres with 5 μM of TDG significantly increased p-GSK-3β (Ser 9) protein expression by 1.15 times ($p = 0.0445$) compared to the control (Fig. 6b). Densitometry readings/intensity ratio of each band in addition to whole blot (uncropped blots) are included in Figures S6 (cells) and S7 (G1 spheres).

Immunofluorescence examination of SH-SY5Y cells and spheres for CD133 stem cell marker expression upon TDG treatment

To validate the inhibitory effect of TDG on neuroblastoma CSCs, we subjected SH-SY5Y cells and G1 spheres to immunofluorescence analysis of CD133 stem cell marker expression (Fig. 7a). Our data revealed that CD133 expression was significantly reduced in both SH-SY5Y cells and spheres (G1) when treated with TDG (Fig. 7b).

TDG inhibited neuroblastoma growth in vivo

To this end, we determined the significant anti-tumor effect of TDG on NB cells in 2D and 3D cultures in vitro. Next, we attempted to assess the potential effect of the drug on NB tumor growth in vivo. So, we injected SH-SY5Y cells subcutaneously into the flanks of NOD-SCID mice in order to generate NB xenografts (Fig. 8a). Average weight of the experimental mice was monitored and was found to be maintained within a normal range, signifying that TDG treatment was well tolerated (Fig. 8b). Treating mice with 20 mg/kg of TDG prompted a robust decrease in NB xenograft tumor growth, reflected by a reduction in tumor volume after 15 days of treatment (Fig. 8c). This shows that TDG reduces NB tumor cell growth in xenograft mouse models.

Discussion

The current study was designed to assess the anti-tumor effects of Tideglusib, an irreversible inhibitor of GSK-3β, on NB-CSCs in vitro and in vivo.

Neuroblastoma is an embryonal solid tumor of the autonomic nervous system that originates from precursor cells of the neural crest tissues and generally affects young children with a median age at diagnosis of 17 months [6, 56, 57]. Treatment strategies that represent the standard of care for most NB patients include surgical resection and
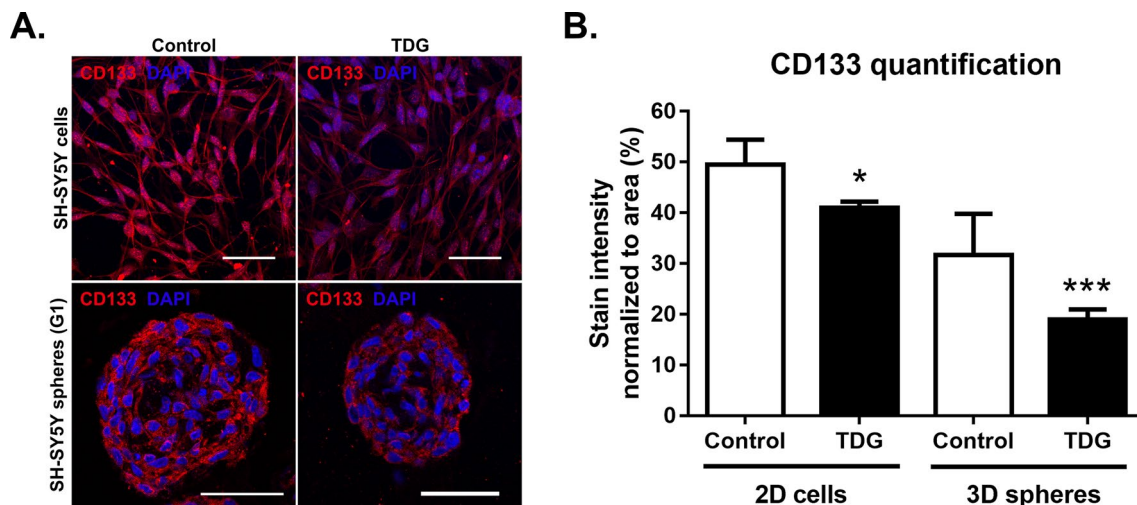

Fig. 7 TDG treatment reduces expression of CD133 stem cell marker in SH-SY5Y cells and spheres. **a** Immunofluorescent images of SH-SY5Y two-dimensional (2D) cells and three-dimensional (3D) spheres (G1) untreated or treated with TDG and stained for CD133 (cancer stem cell marker) and DAPI (nuclear counterstain). Scale bar = 50 μm. **b** Quantification of CD133 expression revealing significant reduction in CD133 expression in both SH-SY5Y cells and spheres (G1) when treated with TDG. Fluorescent signals were captured using a Zeiss LSM 710 laser scanning confocal microscope (Zeiss, Germany) and images were processed using the Zeiss ZEN 2012 image-analysis software. Stain intensity was normalized to area and reported as mean ± SD. Data represent an average of at least three independent experiments (*$p < 0.05$; ***$p < 0.001$; treatment compared to control, student independent t test)
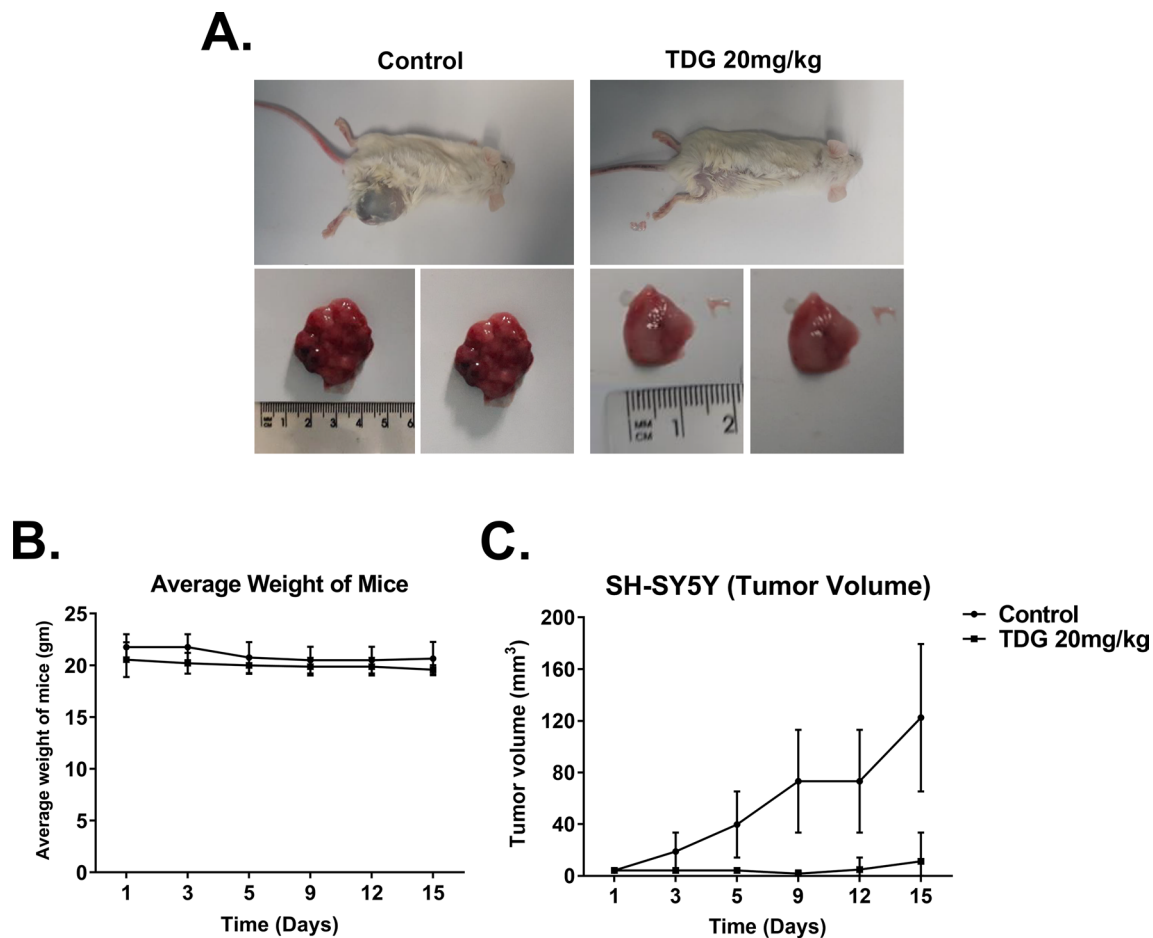
Fig. 8 TDG treatment drastically reduces neuroblastoma tumor burden in xenograft mouse models. 1.2×10^6 SH-SY5Y cells were subcutaneously transplanted in 6- to 8-weeks-old NOD-SCID mice. **a** Images of the subcutaneously generated neuroblastoma xenografts in the control condition vs. treatment with 20 mg/kg TDG. **b** Average weight of mice throughout the experiment was recorded. **c** Tumor size measurements were initiated upon the detection of a palpable tumor post-cell injection. Tumor volume was assessed by direct physical measurements of the tumors at the primary site of injection, every 3 days, until the termination of the experiment. The following general formula was applied: $V = (3.14/6) \times L \times W \times H$; where V is the tumor volume in mm^3, L is the tumor length in mm, W is the tumor width in mm, and H is the tumor height in mm (Wilcoxon matched-pairs signed rank test; data represent an average of $n = 3$ mice; data are reported as median with interquartile range)

chemoradiotherapy [56]. However, in many cases, conventional treatments fail and the tumor recurs due to the presence of dormant slowly dividing cancer stem cells (CSCs) that reside within the tumor bulk. Several studies have identified that CSCs play a crucial role in NB disease progression, relapse, and poor prognosis. A number of pathways have been postulated to contribute to NB-CSC maintenance and chemoresistance including WNT/β-catenin and NOTCH [14, 57]. Therefore, identifying new therapeutic approaches that specifically target NB-CSCs and its related molecular pathways [58] is of high importance to prevent relapse.[9, 58, 59].

Interestingly, GSK-3β represents a common signaling node at the intersection of many of the pathways implicated in NB tumor initiation and progression including Wnt, PI3K/Akt/mTOR, MAPK, NF-κB, and TP53 among others

[24, 28, 44]. Studies suggest a conflicting role of GSK-3β in various human cancers, either as a tumor suppressor or tumor promoter [60]. In NB, it has been shown to provoke an oncogenic role where its inhibition induced cell apoptosis via activating the canonical Wnt signaling pathway in a TP53-independent manner [28]. In line with this study, we showed that GSK-3β was significantly overexpressed in NB tissues relative to other tumor tissues, with a fold change of 1.639, using a publicly available dataset via "Oncomine" research platform (the Neale Multi-cancer Statistics dataset). Various GSK-3β inhibitors have been developed as potential therapeutics for several serious pathologies, including Alzheimer's disease, bipolar disorders, chronic inflammatory processes, and cancer. TDG is a potent, selective and irreversible small molecule non-ATP-competitive GSK-3β inhibitor [22]. Our results showed that TDG significantly

inhibited the proliferation and survival of human NB SH-SY5Y and SK-N-SH cells, in a dose- and time-dependent manner. Results were further validated on IMR-32 human NB cells as well showing consistent inhibitory effect. TDG also significantly reduced migratory ability of SH-SY5Y and SK-N-SH cells. In accordance, Mathuram et al. have previously demonstrated that TDG induced NB cell apoptosis via sub-G0/G1 accumulation and ROS generation [61].

No studies have yet tackled the effect of GSK-3β on NB-CSCs. Since targeting CSCs is essential to overcome therapy resistance, we sought to assess the ability of TDG to target the sub-population of cancer stem/progenitor cells in SH-SY5Y and SK-N-SH cells using 3D Matrigel™-based neurospheres formation assay in vitro [44, 46]. We showed that TDG exhibits a strong inhibitory effect on the self-renewal potential of CSC populations enriched from SH-SY5Y, SK-N-SH and IMR-32 cells suggesting that CSCs are selectively and effectively targeted by TDG. This reduction in sphere-forming ability correlated with the observed decrease in the expression of the stem cell marker CD133. CD133 is a pentaspan transmembrane protein expressed in neural stem cells and its expression was inversely correlated with overall survival of NB patients [62]. CD133 has been indicated as a marker for tumor-initiating cells and silencing CD133 was shown to decrease NB cell colony formation and proliferation, increase differentiation in vitro, and decrease tumor burden in vivo [63]. Studies have shown that CD133+ NB cells efficiently develop tumorospheres, which exhibited high resistance to doxorubicin, cisplatin, carboplatin and etoposide treatment with up-modulation of ABCG2 transporter [14]. Henceforth, we concluded that TDG might serve as an effective therapy in targeting the self-renewal ability of CSCs, a hallmark of cancer progression. Consistent with the in vitro data, SH-SY5Y cells treated with TDG in vivo, drastically reduced the tumorigenic potential of tumor cells.

The anti-tumor role of TDG and its ability to target CSCs could be due to the blockade of the GSK-3β-mediated upregulation of NF-κB-mediated gene transcription [26]. In this context, NF-κB is known to mediate resistance to radiation and chemotherapy in cancer [64, 65]. A study by Duffy et al. showed that GSK3 inhibitors induce apoptosis of NB cells and reduce *MYCN* mRNA levels [28]. Accordingly, GSK-3β inhibitors including TDG could be instigating their efficient anti-tumor role via targeting multi-drug resistant NB cells, and CSCs particularly, and might further re-sensitize those cells that are resistant to conventional therapies. To mention, TDG is now under Phase II Clinical Trials for Alzheimer's disease and for patients with progressive supranuclear palsy. Minimal adverse effects have been reported among patients under study and thus we hypothesized that this drug might carry hope as a novel potential CSCs-targeted therapy for patients suffering from NB [30, 66].

Limitations

We believe our study has several limitations pertaining to the methodology and experimental design. First, we used a limited number of cell lines as in vitro models representing NB and thus more human cell line models for NB could be acquired and tested in future experiments to validate the inhibitory effect of TDG. Also, it is important to assess the effect of TDG on normal neural cells. Second, we mainly relied in our study on experimental assays that serve as functional reporters of the progenitor activity of NB cell lines, as well as the differentiation and self-renewal ability of the stem/progenitor cell population. More studies should follow to evaluate the inhibitory effect of TDG, at a molecular level, and decipher the mechanisms denoting different GSK-3β-related signaling pathways that are entangled in the pathophysiology of NB and its CSCs. This is particularly important since GSK-3β has a double role in pro- and anti-apoptotic pathways [67]. Third, in our study, we studied the inhibitory effect of TDG on neuroblastoma CSCs by subjecting SH-SY5Y cells and G1 spheres to immunofluorescence analysis of CD133 stem cell marker expression. Nevertheless, other stem cell markers are worth considering to be assessed in future studies, such as BMI1. Fourth, the in vivo experiments that we performed are constricted to single time point of treatment commencement. Such experimental design provides only partial information regarding the effectiveness of the drug on different stages of the disease. Henceforth, this point is important to be addressed in future studies.

Conclusion

Conclusively, TDG proved to be effective in inhibiting in vitro and in vivo NB cell growth. It may hence serve as a potential adjuvant therapeutic agent for this aggressive nervous system tumor. Our study supports the notion that targeting NB CSCs via specifically inhibiting GSK-3β may be crucial to halt NB tumor progression.

Author contributions (CRediT author statement) HFB: project administration, supervision, formal analysis, investigation, methodology, writing—original draft preparation, validation. RMC: investigation, methodology, writing—original draft preparation, writing—reviewing and editing, validation. HH: project administration, resources, writing—reviewing and editing, supervision, validation, visualization. JBG, AM and HM: investigation, methodology, writing—original draft

Compliance with ethical standards

Conflict of interest The authors declare that they have no conflict of interest.

Ethics approval All applicable international, national, and/or institutional guidelines for the care and use of animals were followed. This study was approved by the Institutional Animal Care and Utilization Committee (IACUC) of the American University of Beirut. We also followed the ARRIVE guidelines (https://www.nc3rs.org.uk/arrive-guidelines) for animal researches.

Consent to participate Not applicable.

Consent for publication Not applicable.

References

1. Van Arendonk KJ, Chung DH. Neuroblastoma: tumor biology and its implications for staging and treatment. Children (Basel). 2019;6(1):12.
2. Jiang M, Stanke J, Lahti JM. The connections between neural crest development and neuroblastoma. Curr Top Dev Biol. 2011;94:77–127.
3. Nakagawara A, Ohira M. Comprehensive genomics linking between neural development and cancer: neuroblastoma as a model. Cancer Lett. 2004;204(2):213–24.
4. Brodeur GM. Neuroblastoma: biological insights into a clinical enigma. Nat Rev Cancer. 2003;3(3):203–16.
5. Cohn SL, Pearson AD, London WB, Monclair T, Ambros PF, Brodeur GM, et al. The International Neuroblastoma Risk Group (INRG) classification system: an INRG Task Force report. J Clin Oncol. 2009;27(2):289–97.
6. Maris JM, Hogarty MD, Bagatell R, Cohn SL. Neuroblastoma. Lancet. 2007;369(9579):2106–20.
7. Pinto NR, Applebaum MA, Volchenboum SL, Matthay KK, London WB, Ambros PF, et al. Advances in risk classification and treatment strategies for neuroblastoma. J Clin Oncol. 2015;33(27):3008–177.
8. Siegel RL, Miller KD, Jemal A. Cancer statistics. CA Cancer J Clin. 2020;70(1):7–30.
9. Bahmad HF, Chamaa F, Assi S, Chalhoub RM, Abou-Antoun T, Abou-Kheir W. Cancer stem cells in neuroblastoma: expanding the therapeutic frontier. Front Mol Neurosci. 2019;12:131.
10. Frank NY, Schatton T, Frank MH. The therapeutic promise of the cancer stem cell concept. J Clin Investig. 2010;120(1):41–50.
11. Lugli A, Iezzi G, Hostettler I, Muraro MG, Mele V, Tornillo L, et al. Prognostic impact of the expression of putative cancer stem cell markers CD133, CD166, CD44s, EpCAM, and ALDH1 in colorectal cancer. Br J Cancer. 2010;103(3):382–90.
12. Babashah S. Cancer stem cells: emerging concepts and future perspectives in translational oncology. Berlin: Springer; 2015.
13. Ross RA, Spengler BA. Human neuroblastoma stem cells. Semin Cancer Biol. 2007;17(3):241–7.
14. Mahller YY, Williams JP, Baird WH, Mitton B, Grossheim J, Saeki Y, et al. Neuroblastoma cell lines contain pluripotent tumor initiating cells that are susceptible to a targeted oncolytic virus. PLoS ONE. 2009;4(1):e4235.
15. Aravindan N, Jain D, Somasundaram DB, Herman TS, Aravindan S. Cancer stem cells in neuroblastoma therapy resistance. Cancer Drug Resist. 2019;2:948–67.
16. Shohet JM, Ghosh R, Coarfa C, Ludwig A, Benham AL, Chen Z, et al. A genome-wide search for promoters that respond to increased MYCN reveals both new oncogenic and tumor suppressor microRNAs associated with aggressive neuroblastoma. Can Res. 2011;71(11):3841–51.
17. Alisi A, Cho WC, Locatelli F, Fruci D. Multidrug resistance and cancer stem cells in neuroblastoma and hepatoblastoma. Int J Mol Sci. 2013;14(12):24706–25.
18. Khalil MA, Hrabeta J, Cipro S, Stiborova M, Vicha A, Eckschlager T. Neuroblastoma stem cells - mechanisms of chemoresistance and histone deacetylase inhibitors. Neoplasma. 2012;59(6):737–46.
19. Megison ML, Gillory LA, Beierle EA. Cell survival signaling in neuroblastoma. Anticancer Agents Med Chem. 2013;13(4):563–75.
20. Matsui WH. Cancer stem cell signaling pathways. Medicine (Baltimore). 2016;95(1 Suppl 1):S8–S19.
21. Stambolic V, Woodgett JR. Mitogen inactivation of glycogen synthase kinase-3 beta in intact cells via serine 9 phosphorylation. Biochem J. 1994;303(Pt 3):701–4.
22. Wu D, Pan W. GSK3: a multifaceted kinase in Wnt signaling. Trends Biochem Sci. 2010;35(3):161–8.
23. Gupta K, Stefan T, Ignatz-Hoover J, Moreton S, Parizher G, Saunthararajah Y, et al. GSK-3 inhibition sensitizes acute myeloid leukemia cells to 1,25D-mediated differentiation. Cancer Res. 2016;76(9):2743–53.
24. Ougolkov AV, Billadeau DD. Targeting GSK-3: a promising approach for cancer therapy? Fut Oncol (Lond, Engl). 2006;2(1):91–100.
25. Ougolkov AV, Fernandez-Zapico ME, Savoy DN, Urrutia RA, Billadeau DD. Glycogen synthase kinase-3beta participates in nuclear factor kappaB-mediated gene transcription and cell survival in pancreatic cancer cells. Cancer Res. 2005;65(6):2076–81.
26. Walz A, Ugolkov A, Chandra S, Kozikowski A, Carneiro BA, O'Halloran TV, et al. Molecular pathways: revisiting glycogen synthase kinase-3beta as a target for the treatment of cancer. Clin Cancer Res. 2017;23(8):1891–7.
27. Nakada M, Minamoto T, Pyko IV, Hayashi Y, Hamada J-I. The pivotal roles of GSK3β in glioma biology. Molecular targets of CNS tumors. London: IntechOpen; 2011.
28. Duffy DJ, Krstic A, Schwarzl T, Higgins DG, Kolch W. GSK3 inhibitors regulate MYCN mRNA levels and reduce

neuroblastoma cell viability through multiple mechanisms, including p53 and Wnt signaling. Mol Cancer Ther. 2014;13(2):454–67.

29. Eldar-Finkelman H, Martinez A. GSK-3 Inhibitors: preclinical and clinical focus on CNS. Front Mol Neurosci. 2011;4(32).

30. del Ser T, Steinwachs KC, Gertz HJ, Andres MV, Gomez-Carrillo B, Medina M, et al. Treatment of Alzheimer's disease with the GSK-3 inhibitor tideglusib: a pilot study. J Alzheimer's Dis. 2013;33(1):205–15.

31. Dominguez JM, Fuertes A, Orozco L, del Monte-Millan M, Delgado E, Medina M. Evidence for irreversible inhibition of glycogen synthase kinase-3beta by tideglusib. J Biol Chem. 2012;287(2):893–904.

32. Tolosa E, Litvan I, Höglinger GU, Burn D, Lees A, Andrés MV, et al. A phase 2 trial of the GSK-3 inhibitor tideglusib in progressive supranuclear palsy. Mov Disord. 2014;29(4):470–8.

33. Biedler JL, Helson L, Spengler BA. Morphology and growth, tumorigenicity, and cytogenetics of human neuroblastoma cells in continuous culture. Can Res. 1973;33(11):2643–52.

34. Biedler JL, Roffler-Tarlov S, Schachner M, Freedman LS. Multiple neurotransmitter synthesis by human neuroblastoma cell lines and clones. Can Res. 1978;38(11 Pt 1):3751–7.

35. Ross RA, Spengler BA, Biedler JL. Coordinate morphological and biochemical interconversion of human neuroblastoma cells. J Natl Cancer Inst. 1983;71(4):741–7.

36. Tumilowicz JJ, Nichols WW, Cholon JJ, Greene AE. Definition of a continuous human cell line derived from neuroblastoma. Cancer Res. 1970;30(8):2110–8.

37. van Meerloo J, Kaspers GJ, Cloos J. Cell sensitivity assays: the MTT assay. Methods Mol Biol (Clifton, NJ). 2011;731:237–45.

38. Mosmann T. Rapid colorimetric assay for cellular growth and survival: application to proliferation and cytotoxicity assays. J Immunol Methods. 1983;65(1–2):55–63.

39. Riss TL, Moravec RA, Niles AL, Duellman S, Benink HA, Worzella TJ, et al. Cell viability assays. In: Sittampalam GS, Coussens NP, Brimacombe K, Grossman A, Arkin M, Auld D, et al., editors. Assay guidance manual. Bethesda: Eli Lilly & Company; 2004.

40. Riss T, Moravec R, Niles A. Cell viability assays. In: Assay guidance manual [Internet]. Bethesda: Eli Lilly & Company; 2016.

41. Strober W. Trypan blue exclusion test of cell viability. Curr Protoc Immunol. 2001;Appendix 3:Appendix 3B.

42. Rodriguez LG, Wu X, Guan J-L. Wound-healing assay. In: Guan J-L, editor. Cell migration: developmental methods and protocols. Totowa: Humana Press; 2005. p. 23–29.

43. Bahmad HF, Cheaito K, Chalhoub RM, Hadadeh O, Monzer A, Ballout F, et al. Sphere-formation assay: three-dimensional in vitro culturing of prostate cancer stem/progenitor sphere-forming cells. Front Oncol. 2018;8:347.

44. Mouhieddine TH, Nokkari A, Itani MM, Chamaa F, Bahmad H, Monzer A, et al. Metformin and Ara-a effectively suppress brain cancer by targeting cancer stem/progenitor cells. Front Neurosci. 2015;9:442.

45. Abou-Kheir W, Hynes PG, Martin P, Yin JJ, Liu YN, Seng V, et al. Self-renewing Pten−/− TP53−/− protospheres produce metastatic adenocarcinoma cell lines with multipotent progenitor activity. PLoS ONE. 2011;6(10):e26112.

46. Bahmad HF, Mouhieddine TH, Chalhoub RM, Assi S, Araji T, Chamaa F, et al. The Akt/mTOR pathway in cancer stem/progenitor cells is a potential therapeutic target for glioblastoma and neuroblastoma. Oncotarget. 2018;9(71):33549–61.

47. Abou-Kheir W, Hynes PG, Martin PL, Pierce R, Kelly K. Characterizing the contribution of stem/progenitor cells to tumorigenesis in the Pten−/−TP53−/− prostate cancer model. Stem Cells. 2010;28(12):2129–40.

48. Cao L, Zhou Y, Zhai B, Liao J, Xu W, Zhang R, et al. Sphere-forming cell subpopulations with cancer stem cell properties in human hepatoma cell lines. BMC Gastroenterol. 2011;11:71.

49. Chen G, Xu S, Renko K, Derwahl M. Metformin inhibits growth of thyroid carcinoma cells, suppresses self-renewal of derived cancer stem cells, and potentiates the effect of chemotherapeutic agents. J Clin Endocrinol Metab. 2012;97(4):E510–E520520.

50. Hyun KH, Yoon CH, Kim RK, Lim EJ, An S, Park MJ, et al. Eckol suppresses maintenance of stemness and malignancies in glioma stem-like cells. Toxicol Appl Pharmacol. 2011;254(1):32–40.

51. Matsuda K, Sato A, Okada M, Shibuya K, Seino S, Suzuki K, et al. Targeting JNK for therapeutic depletion of stem-like glioblastoma cells. Sci Rep. 2012;2:516.

52. El-Merahbi R, Liu Y-N, Eid A, Daoud G, Hosry L, Monzer A, et al. Berberis libanotica ehrenb extract shows anti-neoplastic effects on prostate cancer stem/progenitor cells. PLoS ONE. 2014;9(11):e112453.

53. Daoud G, Monzer A, Bahmad H, Chamaa F, Hamdar L, Mouhieddine TH, et al. Primary versus castration-resistant prostate cancer: modeling through novel murine prostate cancer cell lines. Oncotarget. 2016;7(20):28961–75.

54. Cheung N-KV, Dyer MA. Neuroblastoma: developmental biology, cancer genomics and immunotherapy. Nat Rev Cancer. 2013;13(6):397–411.

55. Walton JD, Kattan DR, Thomas SK, Spengler BA, Guo H-F, Biedler JL, et al. Characteristics of stem cells from human neuroblastoma cell lines and in tumors. Neoplasia (New York, NY). 2004;6(6):838–45.

56. Maris JM. Recent advances in neuroblastoma. N Engl J Med. 2010;362(23):2202–11.

57. London WB, Castleberry RP, Matthay KK, Look AT, Seeger RC, Shimada H, et al. Evidence for an age cutoff greater than 365 days for neuroblastoma risk group stratification in the Children's Oncology Group. J Clin Oncol. 2005;23(27):6459–65.

58. Abdullah LN, Chow EK-H. Mechanisms of chemoresistance in cancer stem cells. Clin Transl Med. 2013;2:3.

59. Singh SK, Clarke ID, Hide T, Dirks PB. Cancer stem cells in nervous system tumors. Oncogene. 2004;23(43):7267–73.

60. Mills CN, Nowsheen S, Bonner JA, Yang ES. Emerging roles of glycogen synthase kinase 3 in the treatment of brain tumors. Front Mol Neurosci. 2011;4:47.

61. Mathuram TL, Ravikumar V, Reece LM, Karthik S, Sasikumar CS, Cherian KM. Tideglusib induces apoptosis in human neuroblastoma IMR32 cells, provoking sub-G0/G1 accumulation and ROS generation. Environ Toxicol Pharmacol. 2016;46:194–205.

62. Tong QS, Zheng LD, Tang ST, Ruan QL, Liu Y, Li SW, et al. Expression and clinical significance of stem cell marker CD133 in human neuroblastoma. World J Pediatr. 2008;4(1):58–62.

63. Takenobu H, Shimozato O, Nakamura T, Ochiai H, Yamaguchi Y, Ohira M, et al. CD133 suppresses neuroblastoma cell differentiation via signal pathway modification. Oncogene. 2011;30(1):97–105.

64. Aggarwal BB. Nuclear factor-kappaB: the enemy within. Cancer Cell. 2004;6(3):203–8.

65. Tas SW, Vervoordeldonk MJ, Tak PP. Gene therapy targeting nuclear factor-kappaB: towards clinical application in inflammatory diseases and cancer. Current Gene Ther. 2009;9(3):160–70.

66. Lovestone S, Boada M, Dubois B, Hull M, Rinne JO, Huppertz HJ, et al. A phase II trial of tideglusib in Alzheimer's disease. J Alzheimer's Dis. 2015;45(1):75–88.

67. Jacobs KM, Bhave SR, Ferraro DJ, Jaboin JJ, Hallahan DE, Thotala D. GSK-3β: a bifunctional role in cell death pathways. Int J Cell Biol. 2012;2012:930710.

Affiliations

Hisham F. Bahmad[1,2,5] · Reda M. Chalhoub[1,6] · Hayat Harati[2] · Jolie Bou-Gharios[1,2] · Sahar Assi[1] · Farah Ballout[1] · Alissar Monzer[1] · Hiba Msheik[1] · Tarek Araji[1] · Mohamad K. Elajami[1,7] · Paola Ghanem[1] · Farah Chamaa[1] · Humam Kadara[3] · Tamara Abou-Antoun[4] · Georges Daoud[1] · Youssef Fares[2] · Wassim Abou-Kheir[1]

Wassim Abou-Kheir
wa12@aub.edu.lb

1. Department of Anatomy, Cell Biology and Physiological Sciences, Faculty of Medicine, American University of Beirut, Beirut, Lebanon

2. Neuroscience Research Center, Faculty of Medicine, Lebanese University, Beirut, Lebanon

3. Department of Translational Molecular Pathology, The University of Texas MD Anderson Cancer Center, Houston, TX, USA

4. School of Pharmacy, Department of Pharmaceutical Sciences, Lebanese American University, Byblos, Lebanon

5. Present Address: Arkadi M. Rywlin M.D. Department of Pathology and Laboratory Medicine, Mount Sinai Medical Center, Miami Beach, FL, USA

6. Present Address: Medical Scientist Training Program, College of Medicine, Medical University of South Carolina, Charleston, SC, USA

7. Present Address: Department of Internal Medicine, Mount Sinai Medical Center, Miami Beach, FL, USA